Journal of Computer-Aided Molecular Design, **13:** 297–313, 1999.
KLUWER/ESCOM

The structural and electronical factors that contribute affinity for the time-dependent inhibition of PGHS-1 by indomethacin, diclofenac and fenamates

R. Pouplana, C. Pérez, J. Sánchez[a], J.J. Lozano[b] & P. Puig-Parellada[a]
Departament de Farmàcia, Unitat Fisicoquímica, Facultat de Farmàcia, Universitat de Barcelona, Av. Joan XXIII, s/n, E-08028 Barcelona, Spain; Present addresses: [a]*Unitat de Farmacología, Facultat de Medicina, Universitat de Barcelona, c/ Casanovas 143, E-08008 Barcelona, Spain;* [b] *Departament de Informàtica Medica (IMIM), Facultat de Medicina (UAB), c/ Doctor Aiguader 80, E-08003 Barcelona, Spain*

Received 20 April 1998; Accepted 14 September 1998

Key words: anti-inflammatory agents, cyclooxygenase inhibitors, fenamates, PGHS-1, QSAR modeling

Summary

PGHS-1 and PGHS-2 are the targets of nonsteroidal anti-inflammatory drugs (NSAIDs). It appears that the high degree of selectivity for inhibition of PGHS-2 shown by certain compounds is the result of two mechanisms (time-dependent and time-independent inhibition), by which they interact with each isoform. The fenamic acids can be divided into competitive inhibitors of substrate binding and competitive inhibitors that cause time-dependent losses of cyclooxygenase activity. The cyclooxygenase activity was measured by oxygen consumption following preincubation of the enzyme and the inhibitor for increasing periods of time. The rate constants associated with binding inhibition kinetics and structure-activity relationships were calculated for a large number of fenamates, diclofenac and indomethacin. The K_I^* values are similar but the individual rate constants are markedly different: K_I is two-fold lower, and k_2 is six-fold slower for diclofenac than for indomethacin. All the active time-dependent compounds show MEPs with a negative conical surface, with their vertex on the minimum of the carboxyl group, which extends around the first aromatic ring to the central region. The conical surface keeps an open angle of 61° or larger, and a close contact surface with the residues Ala^{527}, $Ileu^{523}$, Val^{349}, and Ser^{530}, in the zones surrounding the bridging amino group and the chlorine atoms for meclofenamate and diclofenac, or in the region around the carbonyl group for indomethacin. The K_I^* and IC_{50} values indicate that the interactions that promote the slow binding kinetics must be examined in relation to the reaction energies of formation (ΔH_r) of an ionic bond between the deprotonated carboxylic acid group of acid NSAIDs with the monocationic guanidinum group of Arg^{120}, the free energies of solvation in aqueous solution, and the molecular volumes measured. Presumably indomethacin, diclofenac and meclofenamate cause the enzyme to undergo a subtle conformational change to a form that binds compounds even more tightly, with some slight structural changes confined to reorientations of the Arg^{277} and Gln^{358} side chains. These results show that the model has reliably chosen regions of biological significance consistent with both the X-ray crystallographic and kinetic results.

Introduction

Prostaglandins act as potent mediators of pain, fever and inflammation. Recent human epidemiologic studies suggest an inverse relationships between intake of nonsteroidal antiinflammatory drugs (NSAIDs) and the risk of colorectal cancer [1,2]. The prostaglandin H synthase (PGHS) catalyzes the first step in the conversion of arachidonate to the prostaglandin endoperoxides PGG_2 then PGH_2. Two isoforms of PGHS have been identified [3,4]. The first, PGHS-1, is constitutively expressed in most tissues and is believed to generate prostaglandins for normal physiological functions. The second isoform, PGHS-2, is charac-

terized by a rapid induction by a variety of stimuli, including mitogens, hormones, cytokines, and growth factors. Both isoforms have been shown to be the target of nonsteroidal anti-inflammatory drugs (NSAIDs) [5,6]. At least three types of NSAID-mediated inhibition of PGHS isoforms have been reported. Firstly, aspirin irreversibly inhibits prostaglandin production of PGHS-1. Secondly, NSAID-mediated inhibition is time-dependent, without resultant covalent modification. In the third type of NSAID-mediated inhibition, compounds act as time-independent, reversible inhibitors. Furthermore, three distinct but similar kinetic mechanisms for the inhibition of PGHS-2 have been identified. It appears that the high degree of selectivity for inhibition of PGHS-2 shown by certain compounds is the result of the two different mechanisms (time-dependent, time-independent inhibition), by which it interacts with each isoform [7].

The fenamates and structures related to the fenamic acids are N-arylated derivatives of anthranilic acid or 2-aminonicotinic acid, which are a family of potent analgesic antiinflammatory drugs [8]. The fenamic acids can be classified as competitive inhibitors of substrate binding and competitive inhibitors that cause time-dependent losses of cyclooxygenase activity. The major drawback in the use of these compounds is their toxicity. Understanding the interaction of NSAIDs with PGHS can provide insight which may contribute to the development of NSAIDs with enhanced therapeutic potential and lower toxicity.

Surprisingly, meclofenamate, diclofenac and indomethacin show a rapid time-dependent inhibitory effect. Thus, it seems that geometrical similarity is not a sufficient criterion to explain the time-dependent/time-independent inhibition of PGHS-1 by these compounds, and that other properties should be included in the model for a more realistic description of the recognition process.

The knowledge of molecular electrostatic potential (MEP) distributions makes it possible to interpret and predict reactive properties in different contexts, from chemical reactivity to biological recognition. The recent determination of the refined X-ray crystal structures of the complexes of ovine PGHS-1 with iodosuprofen and iodoindomethacin has led to the development of a model for the topography of the NSAID binding site in PGHS-1 [9–11]. This paper presents a summary of the results of the rate constants associated with binding inhibition kinetics (K_I^*, IC_{50}) and structure-activity relationships defined for a series of fenamates, diclofenac and indomethacin.

Docking the NSAID compounds in the long hydrophobic channel of the proposed active site of PGHS-1 shows that only the compounds that adopt almost perpendicular arrangement between the aromatic rings, by conferring conformational rigidity, and produce, in the space around the first aromatic ring, a very deep region of attractive potential to an approaching electrophile, and show a bulky positive region of MEP in the upper zone are the time-dependent inhibitors.

This study provides evidence of the importance of the Arg^{120} residue in PGHS-1 for interaction with NSAIDs containing a free carboxylic-acid moiety. The results of the rate constants associated with inhibition kinetics (K_I^* and IC_{50}) indicate that the interactions that promote the slow binding kinetics must be examined in relation to the reaction energies of formation (ΔH_r) of an ionic bond between the deprotonated carboxylic acid group of acid NSAIDs with the monocationic guanidinum group of Arg^{120}, the free energies of solvation in aqueous solution, and the molecular volumes measured.

Materials and methods

Experimental

Materials. Haemin, phenol, and other reagents were from Sigma. The PGHS-1 was purified to homogeneity from ovine seminal vesicles [12] and reconstitued by addition of excess haemin. Arachidonic acid and ovine PGHS-1 standard were purchased from Cayman Chemical Co. Indomethacin, meclofenamic, mefenamic, flufenamic and niflumic acids, and diclofenac were obtained from Sigma. Clonixin [13] was a gift from Sanofi-Winthrop, S.A. The buffer used for all incubations consisted of 0.1 M Tris-HCl pH 8.5 containing 1 mM phenol unless otherwise stated.

Cyclooxygenase activity. The oxidation of arachidonic acid to prostaglandin H_2 by PGHS is associated with the consumption of 2 mol of oxygen for every mol of product formed. The continuous progress of the reaction can be measured by monitoring the consumption of oxygen. The time dependency of inhibition of PGHS-1 by these NSAIDs was studied by preincubation of the enzyme (2.5 kU/mg) in the presence of drug for increasing periods of time (0–30 min) before initiation of the reaction. The final inhibitor concentrations used were 0, 0.1, 0.2, 0.3, 5, 10, 15, 20, 30 and 50 μM (0, 0.05, 0.4 and 0.5 in some experiments). The reactions were initiated with 250 μM

arachidonic acid, after preincubation with either inhibitor, a concentration greater than 50-fold excess of the apparent K_m. Under these conditions, all enzyme-inhibitor complexes that are in rapid equilibrium with free enzyme should rapidily bind the excess substrate and catalyze product formation. The inhibition will be the result of enzyme-inhibitor complex that is not in rapid equilibrium with free enzyme and there is a linear relation between the consumption of arachidonate and the consumption of oxygen throughout the range examined [38].

Oxygen consumption was measured at 37 °C on a YSI model 5300 Oxygen Monitor equipped with two oxygen electrodes. Continuous recording were made on a dual channel recorder with one channel recording the oxygen consumption by enzyme (activity control) in the chambers and the other channel recording the oxygen consumption by preincubating enzyme-inhibitor in the chamber. The analogue output was collected and transformed to a digital signal using an external connection to a Data Translation DT01 data system. The final volume in the sample chamber was usually 2.0 ml, and the maximum volume of all additions during an assay was 0.15 ml. The maximum initial velocity was determined from a first derivative spectrum of the first minute of the oxygen consumption curve. The average of the 5 minimum points was used to determine the maximum initial velocity. Each experiment was repeated at least twice.

A mathematical model was developed by Callan et al. [14], resulting in a final three-parameter equation describing the initial maximum velocity of the enzyme-substrate reaction as a function of the enzyme-inhibitor preincubation time. The mathematical interpretation of the theoretical kinetic model is subject to two phases, a preincubation phase in which inhibitor is incubated with enzyme in the absence of substrate, and a reaction phase, which begins when the substrate is added to the inhibitor enzyme mixture.

The reaction of product formation is initiated by adding substrate after T seconds of preincubation, and the following dynamics are assumed where *E*, *I*, *EI*, *EI**, *S*, *P*, and E_i describe the concentration of free enzyme, free inhibitor, enzyme-inhibitor complex, and isomerized enzyme-inhibitor complex with time-dependent inhibition at time t, substrate, product and inactivated enzyme, respectively.

$$EI^* \underset{k_2}{\overset{k_{-2}}{\rightleftharpoons}} EI \underset{Ik_1}{\overset{k_{-1}}{\rightleftharpoons}} E \underset{k_{-3}}{\overset{Sk_3}{\rightleftharpoons}} \underset{E_i}{\overset{\dot{E}S \downarrow k_5}{}} \overset{k_4}{\rightarrow} P + E$$

The equation for the maximum velocity after T seconds of preincubation as a percent of control is:

$$f(t) = 100Q[1 - \frac{k_{app}}{k_{app} + k_{-2}}(1 - e^{(k_{app}+k_{-2})^T})] \quad (1)$$

where

$$Q = \frac{1 + \frac{K_m}{S}}{1 + \frac{K_m}{S}(1 + \frac{I}{K_I})} \quad (2)$$

and

$$k_{app} = \frac{k_2}{1 + \frac{K_I}{I}} \quad (3)$$

The time-velocity curves were obtained for various inhibitor concentrations, and the three parameters and their asymptotic standard errors were estimated by simultaneously fitting the time-velocity curves for several inhibitor concentrations to Equation 1 ($r^2 > 0.990$). The apparent K_m value used for data analysis was 5 μM. The Nelder-Mead algorithm was used to estimate the parameters. The values of k_2, k_{-2}, and K_I ($K_I = k_{-1}/k_1$) for each time-dependent inhibitor were determined by computer-fitting the values of k_{app} for each concentration to Equation 3.

The overall affinity of a slow binding inhibitor (K_I^*) is defined by the following equation:

$$K_I^* = K_I \frac{k_{-2}}{k_2} \quad (4)$$

The preparations of PGHS-1 were preincubated with varying concentrations of inhibitor for 30 min followed by the initiation of the reaction with 250 μM arachidonic acid and the inhibition of the initial rate of oxygen consumption was determined. The results were plotted as percentage of inhibition of PGHS activity versus inhibitor concentration. The IC_{50} (concentration of NSAID that causes 50% decrease in enzyme activity) values were determined using a 2-parameter logistic fit ($r^2 > 0.985$). The IC_{50} correspond to the K_I^* values.

Molecular modeling

The molecular modeling was carried out on a 4D/TG35 Silicon Graphics computer using the Biosym/MSI molecular modeling software. Molecular geometries (Figure 1) of indomethacin, diclofenac,

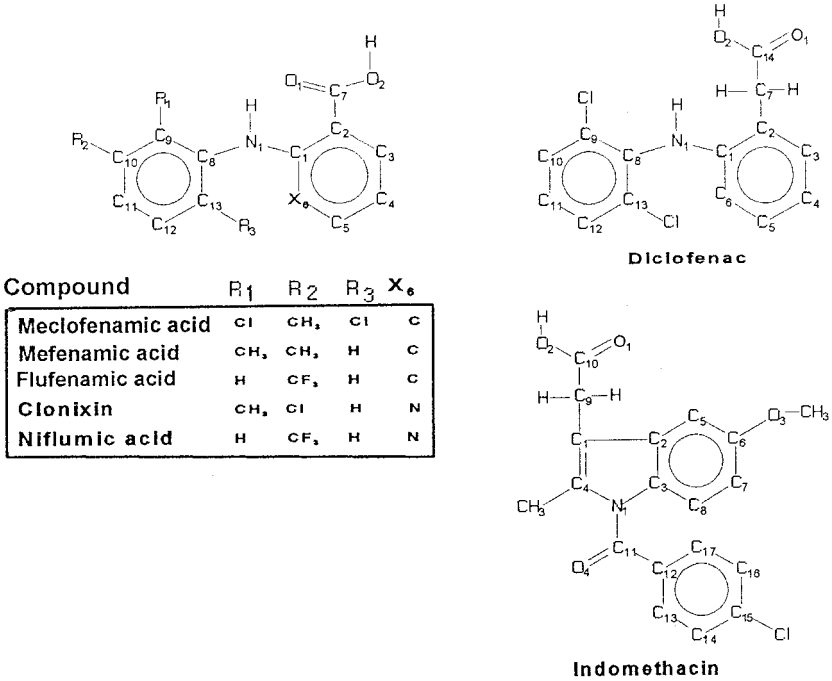

Compound	R_1	R_2	R_3	X_6
Meclofenamic acid	Cl	CH_3	Cl	C
Mefenamic acid	CH_3	CH_3	H	C
Flufenamic acid	H	CF_3	H	C
Clonixin	CH_3	Cl	H	N
Niflumic acid	H	CF_3	H	N

Figure 1. Structural comparison and the numbering scheme of clonixin, flufenamic acid, mefenamic acid, meclofenamic acid, niflumic acid, diclofenac and indomethacin.

niflumic, meclofenamic, flufenamic and mefenamic acids were obtained from crystallographic data and conformational analysis [15–17].

For the other compound, clonixin (2-(2′ methyl-3′ chloro anilino) nicotinic acid) [13], conformational analysis was performed by means of a molecular-mechanics method using the conjugate algorithm of the DISCOVER program [18]. The geometries of lowest energy obtained by a systematic search of two dihedral angles were all optimized by the AM1 method, using the MOPAC 6.0 program [19].

The free energies of solvation in aqueous solution were obtained for all anion (charge $= -1$) compounds from the active conformations by the AM1-SM2 solvation model, using the AMSOL 5.4.1 program [20].

The electrostatic potential V generated at a point r_i for a molecular system with electron density function ρ(r) is given by

$$V(r_i) = \sum_A \frac{Z_A}{|r_i - R_A|} - \int \frac{\rho(r)}{|r_i - r|} dr \qquad (5)$$

where $\mathbf{Z}_A$ is the charge on nucleus **A**, located at $\mathbf{R}_A$.

The Gaussian-94 software package [21] was used in ab initio computations. The molecular electronic wavefunction we used to calculate the MEP was obtained in the framework of the HF-SCF method by ab initio split-valence basis set (3–21G*) computation. The MEP minima values were found with the MEPMIN program [22].

Several topological characteristics of the MEP, minima energies and locations were determined for each molecule from the wavefunctions computed using the basis set detailed above. The isopotential surfaces in the 3D space at different V values were obtained using the interpolation technique of the Insight II program v. 2.3 [18].

In addition, the AutoDock 2.4 program [23] was used to locate binding modes for a specified ligand of know 3D structure in a target PGHS-1 protein. This method predicts optimal modes of interaction of a flexible small molecule with a rigid macromolecular target. Two sets of experiments were performed. The first set was designed to test AutoDock's ability to predict binding modes and to determine whether a simulated annealing algorithm could reproduce the X-ray crystal structure observed experimentally, in a representative variety of NSAID-PGHS-1 situations.

We chose the 3.5 Å structure of the complex of ovine PGHS-1 with bromoaspirin, the PGHS-iodosuprofen complex structure (refined at 3.5 Å to an R-value of 0.189) and PGHS-iodoindomethacin complex structure for the cis and trans models (refined at

4.5 Å to an R-value of 0.254). Crystallographic coordinates were taken from the Brookhaven Protein Data Bank.

The crystal structures have provided a framework in which to dock structurally related ligands. Surprisingly, a comparison of 3D structures of these X-ray crystal structures of PGHS-1 complexed with different NSAIDs indicated a similar topology, with slight structural changes confined to reorientations of the Arg^{277} and Gln^{358} side chains. However, as iodoindomethacin is much larger than the bromoaspirin (25 vs. 14 non-hydrogen atoms) it is unlikely to be able to bind without a drastic enlargement of the active site.

The second set of docking experiments explored indomethacin, diclofenac and fenamates in the active site of the PGHS-1 crystal structure from the PGHS-iodoindomethacin complex, PGHS-iodosuprofen, and PGHS-bromoaspirin complexes, respectively. The carboxylate oxygen of the NSAIDs was deprotonated, because at physiological pH the carboxyl group became ionized. Six affinity grids were calculated for the enzyme. A hundred simulations with each of the grids were carried out with each NSAID initially oriented facing outside the binding region. The dielectric constant was set at $4r$ to represent a partially solvated state. A simulation consisted of 50 cycles, each of which was carried out at constant temperature (310 K) and contained a multitude of steps. From the 100 simulations with each compound, the binding mode with the lowest interaction energy was evaluated by visual display for favourable contacts in the cyclooxygenase binding site. Optimizations were performed using the DISCOVER force field. Hydrogen bonds were identified by distances between heavy atoms (X-Y cutoff < 3.5 Å) and the XH-Y angle ($> 90°$). The close contacts between two molecules (inhibitor and residues in the active site of PGHS-1) were considered when two atoms are separated by less than 90% of the sum of their van der Waals radii.

The program GRID was used to explore the most relevant regions of the target in the active site of PGHS-1 for selective interactions. GRID [24,25] is a computational procedure for detecting energetically favourable binding sites on molecules of known 3D structure. The energies were calculated as Lennard-Jones, electrostatic, and hydrogen bond interactions between a small chemical group (probe) and the 3D structures (targets), using a position-dependent dielectric function to modulate the strong electrostatic interaction between charged centers.

The GRID origin and axes were chosen such that all the atoms of the target structures were included when they were maintained in the conformation when bound to the protein and an additional region which would include several active site residues of PGHS-1 although the protein residues were not explicitly included in the calculations.

The probes selected for this study include the methyl group (C3), a hydroxyl group bonded to an aromatic system (OH), an sp^2 NH group with lone pair (NH=) and the sp^2 cationic NH_2 group (N2=). The C3 probe has the electronic properties of an sp^3 carbon atom and the GRID parameters for this probe assume that it does not interact electrostatically with the target or form hydrogen bonds. The electronic configuration of the OH probe is defined such that it interacts with the π-system of the aromatic ring, and it makes strong hydrogen-bonding interactions. The energy calculations were performed using 0.5 Å spacing between the grid points in a rectangular box measuring $16 \times 16 \times 17$ Å. They give precise spatial information, and this specificity and sensitivity are an advantage since the probes may then be representative of the important chemical groups present in the active site, provided that the analysis can distinguish between different types of interaction.

Finally, to determine the ionic interaction between the deprotonated carboxylic acid group of acid NSAIDs and the monocationic guanidinum group of Arg^{120} in the active site conformations, the ab initio (3-21G*) reaction enthalpies (ΔH_r) for the formation of an ionic bond with geometry optimization, were calculated.

Results

Inhibition of PGHS-1 by NSAIDs

The oxygen consumption profile is characterized by a rapid, protein-dependent decrease in oxygen concentration after addition of the substrate, arachidonic acid. The maximum velocity associated with oxygen consumption was observed to decrease in a time-dependent manner following preincubation of indomethacin, meclofenamic and diclofenac, with ovine PGHS enzyme. Plots of the percentage activity remaining versus preincubation time show a sharp initial decrease in activity, which eventually reaches a plateau, the amount of activity remaining at saturation is 0.7, 0.75 and 3%, respectively (Figure 2). The

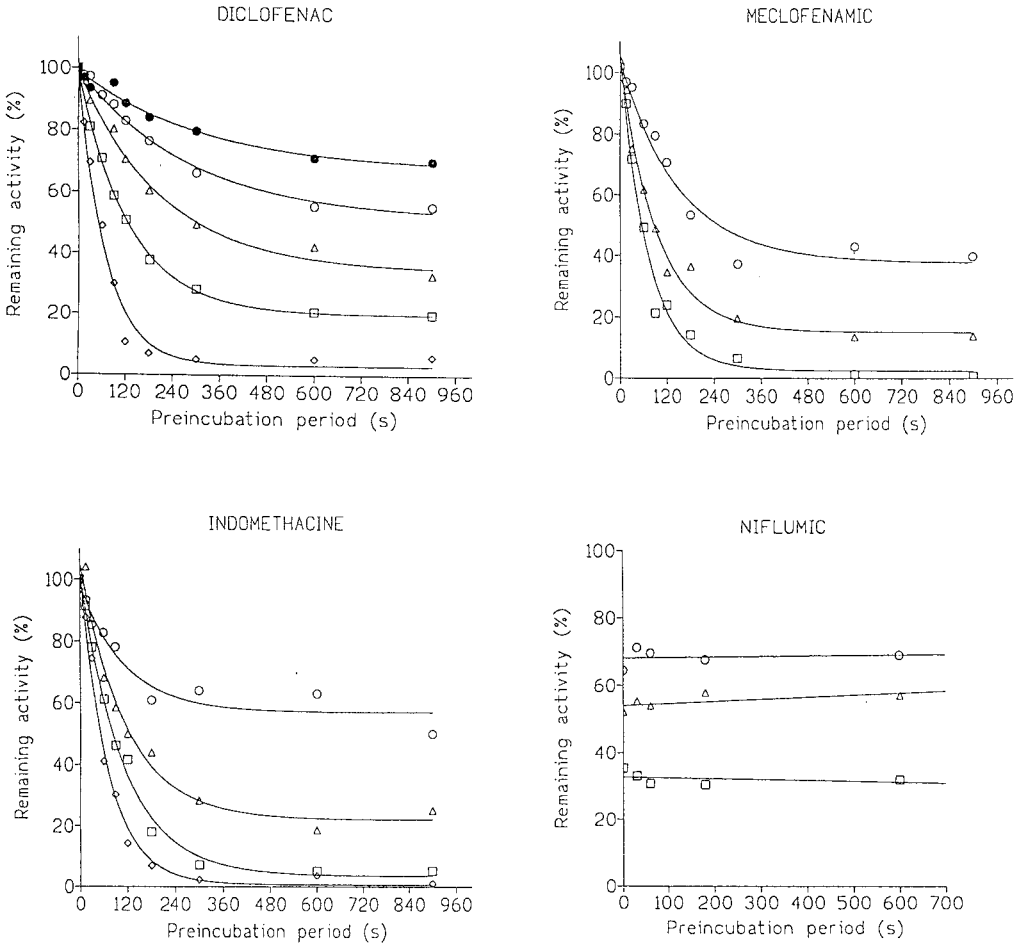

Figure 2. Time course for time-dependent inhibition of ovine PGHS-1 cyclooxygenase activity by indomethacin (○ 100 nM, △ 200 nM, □ 300 nM, ◇ 400 nM), meclofenamic (○ 100 nM, △ 200 nM, □ 300 nM) and diclofenac (○ 50 nM, ○ 100 nM, △ 200 nM, □ 300 nM, □ 500 nM). Time-independent inhibition of ovine PGHS-1 by niflumic (○ 15 μM, △ 30 μM, □ 50 μM). Individual data points were determined from the first derivative of the oxygen consumption assay after preincubation of enzyme with inhibitor for the specified time. Data are represented as a percentage of the remaining control activity. The curves represent the fit (r^2>0.990) of the data at each inhibitor concentration over several experiments to the three-parameter Equation 1.

Table 1. Rate constants (± standard errors) associated with indomethacin, diclofenac and meclofenamic acid inhibition of PGHS-1

Inhibitor	k_2 (s^{-1})	k_{-2} (s^{-1})	K_I (μM)	K_I^* (μM)
Indomethacin	0.45±0.07	0.0032±1E–3	10.9±2.5	0.078±0.005
Diclofenac	0.08±6E–3	0.0024±2E–4	4.3±1.3	0.130±0.005
Meclofenamic	0.38±0.02	0.0035±2E–4	11.7±3.0	0.108±0.003

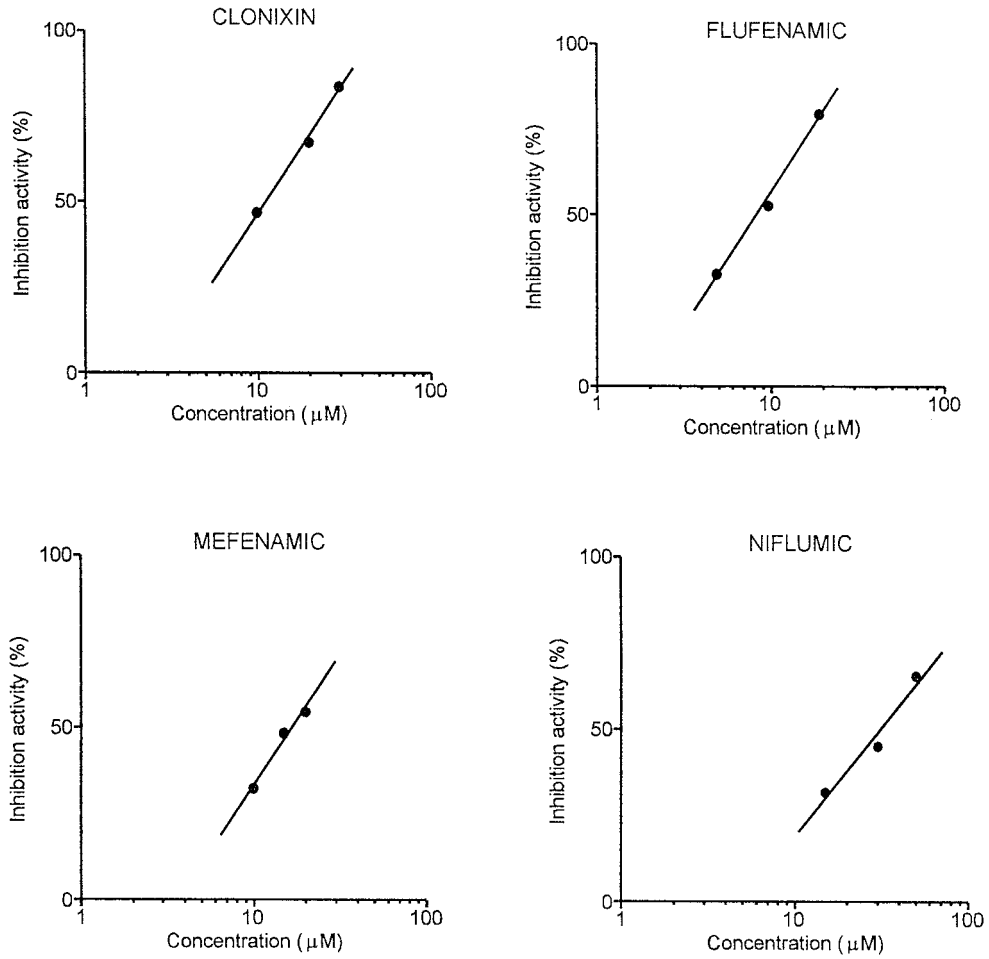

Figure 3. Time-independent inhibition of ovine PGHS-1 cyclooxygenase activity by flufenamic, mefenamic, clonixin and niflumic. The IC_{50} values were determined using a two-parameter logistic fit ($r^2 > 0.980$).

estimated rate constants k_2, k_{-2}, and K_I are shown in Table 1. The overall inhibition K_I^* is defined by Equation 4.

Comparison of the inhibitors shows that all kinetic parameters must be examined in order to understand which factors contribute to the overall affinities. The K_I^* values for indomethacin, diclofenac and meclofenamic (78, 130 and 108 nM, respectively) should show a similar inhibitory potency against PGHS-1. However, the individual rate constants are markedly different: the rate constant for the forward isomerization, k_2, into the second reversible complex EI^*, is six-fold slower for diclofenac, but the dissociation rates, k_{-2}, are similar. Since the efficiency of inhibition is a function of k_2/K_I, an increase in inhibitor potency could be achieved by a compound having a high k_2 value and a low K_I value. The closeness of the rate constants values may indicate that indomethacin and meclofenamic interact initially with the same degree of inhibition but show different time-dependent inhibition from diclofenac. A good correlation was observed between the results and the K_I^* and K_I values reported by Callan et al. [14] and Kulmacz et al. [26] for the inhibition of human PGHS-1 by indomethacin.

These results show that diclofenac was bound tighter to the initial EI complex than the other compounds. The rates of the forward isomerization to EI^* were higher for indomethacin and meclofenamic, although the rate of dissociation from EI^* was similar for diclofenac and the other compounds.

Mefenamic, flufenamic and niflumic acids and clonixin were preincubated for various times (0–30 min) with PGHS-1 at the indicated inhibitor concentrations prior to initiation of the reaction with arachi-

Table 2. The IC_{50} values (± standard errors) determined by inhibiton with 30 min incubation of ovine PGHS-1 by fenamates

Inhibitor	IC_{50} (μM)
Clonixin	14.6±2.4
Flufenamic acid	9.96±2.0
Mefenamic acid	18.5±3.6
Niflumic acid	32.8±6.0

donic acid. The results of these experiments demonstrate that these compounds, at the concentrations used, inhibit ovine PGHS-1 in a time-independent manner (Figure 2). The inhibition of PGHS activity versus inhibitor concentration plots are shown in Figure 3. As shown in Table 2, relative to flufenamic acid (IC_{50} = 9.96 μM), the estimated efficiencies of inhibition of the compounds tested were: clonixin 0.7, mefenamic acid 0.5, and niflumic acid 0.3.

Molecular modeling

Molecular electrostatic potential maps

Fenamates and diclofenac

Figure 4 illustrates the topological features of 3D isopotential maps obtained using ab initio calculations, showing the overall shape of the MEP at the constant V value of -20 kcal mol^{-1}(isopotential surfaces) and -10 kcal mol^{-1} (isopotential contours). Analysis of the equipotential surfaces shows that the MEP negative region extends over the carboxyl and amino groups, while that the other minima exhibit an extended negative region on the first or second aromatic ring. The isopotential surfaces for meclofenamic and diclofenac localize an extended negative region around N1 and the chlorine atoms, with two relative minima at the sides of the N1-H bond. It should be noted that the distance between the minimum and the N1 atom is larger than in the other molecules.

The effect of modifying the meclofenamic and diclofenac structures is also of interest. These compounds are the only molecular structures that adopt almost perpendicular arrangement between the aromatic rings (75° and 69°, respectively), because the chlorine atoms cause maximal twisting of the phenyl ring, and could show a better fit to the receptor [27,28].

For mefenamic and flufenamic, the two phenyl rings are oriented at 50° and 44°, respectively. Furthermore, in flufenamic there is an isolated negative region in the terminal part of the 3D map, corresponding to the relative minimum on fluorine.

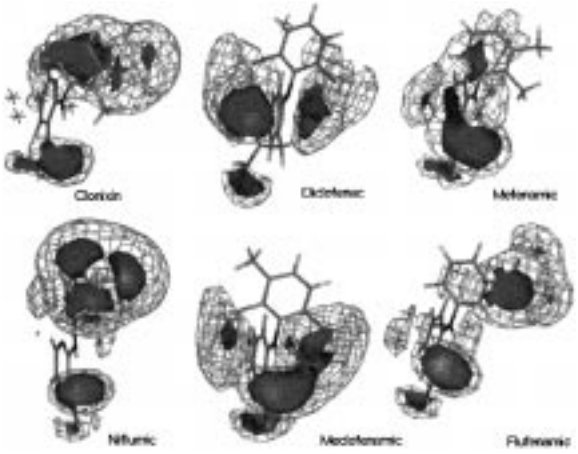

Figure 4. 3D MEP representations calculated with 3-21G. Isopotential surfaces at -20 kcal/mol and isopotential lines at -10 kcal/mol are given.

Niflumic and clonixin are the only fenamates which can adopt a near coplanar arrangement between the aromatic rings and localize an isolated negative region near the nitrogen atom in the first ring. Niflumic shows an extended negative region in the terminal part of the 3D map, corresponding to the three relative minima on fluorines. The extended negative region on the terminal fragment present in flufenamic, niflumic and clonixin allows a stronger interaction with the secondary binding site.

As shown in Figure 5, the global superimposition based on the fitting of the common negative regions of the electrostatic potential, for all fenamates, yields good overlapping. These isopotential contours at -20 kcal mol^{-1} are always localized around the carboxylic group and in the region surrounding the C10 substituent. In contrast, we found that the isopotential surfaces at -20 kcal mol^{-1} are very different in active time-dependent compounds, characterized by a significant hook-shaped protrusion. Meclofenamic and diclofenac had an additional highly negative region around the bridging amino group and the chlorine atoms, with the global minimum close to the carboxylic O1 atom, and a positive long-range electrostatic potential in the region surrounding the C10 substituent. The affinity of the drug for the enzyme may be higher if there are two hydrophobic structures that are not coplanar, and thus enable dual binding.

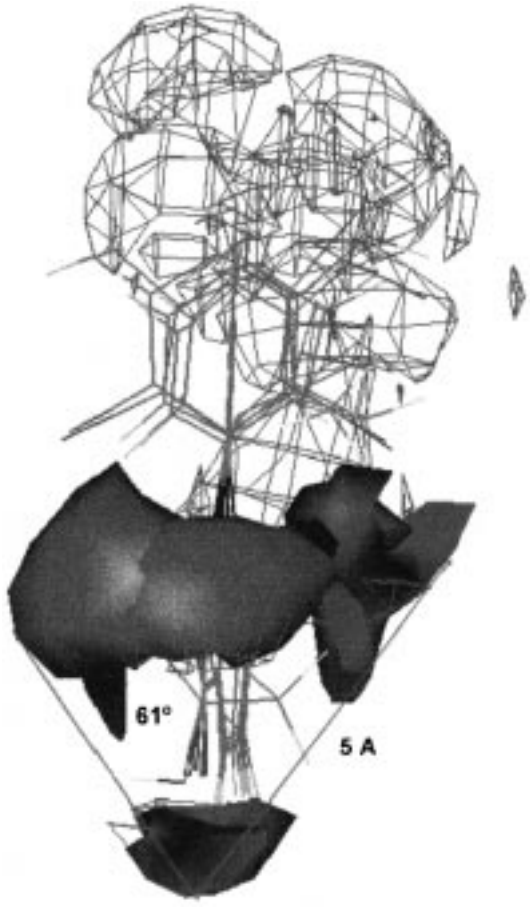

Figure 5. Global superposition of fenamates and diclofenac. Isopotential contours at −20 kcal/mol for 3D MEP are shown. Solid surfaces are negative potentials for meclofenamic and diclofenac; linear surfaces are negative potentials for clonixin, flufenamic, mefenamic and niflumic.

The relationships, if any, between activity and the electrostatic potential values are based on small energy differences in the negative region around the carboxylic group.

Indomethacin

There are only five conformationally significant bonds in the indomethacin about which free rotation should be possible, and so the conformational space available to the molecule is not large. The benzoyl ring can adopt either a *cis* or a *trans* conformation with respect to the indole. These conformers are distinguished by a 180° rotation about the amide bond. In studies of arginine-carboxylate interactions in crystal structures [11], geometrical arguments favour the *cis* model over the *trans.*

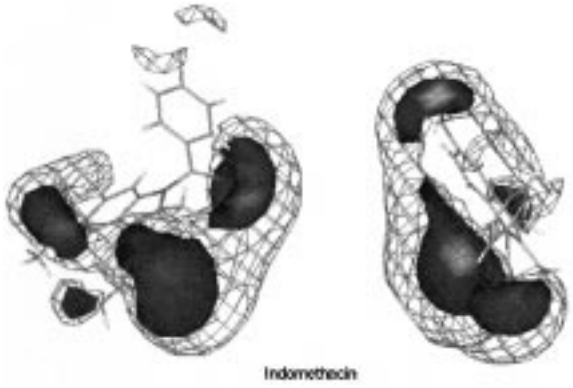

Figure 6. 3D MEP representations calculated with 3–21G for indomethacin in the transverse and longitudinal views. Isopotential surfaces at −20 kcal/mol and isopotential lines at −10 kcal/mol are given.

The MEP topologies for the *cis*-indomethacin (crystallographic data) localize an extended region characterized by positive values of MEP on the whole molecule and three negative potential zones in the lateral regions. The depths of the three global minima are very similar. The relative minima are on the phenyl ring and in the region surrounding the chlorine atom.

The corresponding 3D map (Figure 6) for the *cis*-indomethacin showed a positive long-range electrostatic potential in the phenyl region and the negative isopotential surfaces (-20 kcal mol^{-1}) surrounding the global minima at the carboxyl group and the carbonyl bridge between the phenyl and indole rings that are extended to the upper left quadrant around the methoxy group. The MEP topology is very similar to that of meclofenamic and diclofenac. The isopotential contours at -10 kcal mol^{-1} present similar shape, characterized by a significant hook-shaped protrusion which extends below the plane of the indole ring and ends just above it.

X-ray crystal structure/comparison with the docking model

The X-ray crystal structures clearly indicated that major structural changes had occurred in the enzyme upon binding of iodoindomethacin. The PGHS-1 structure revealed differences of volume in the active site of the enzyme (988.7 Å^3, 1113.9 Å^3 and 1192.1 Å^3, for bromoaspirin, iodosuprofen and iodoindomethacin, respectively), possibly due to packing differences between protein and these inhibitors. The enzyme active site in the PGHS-

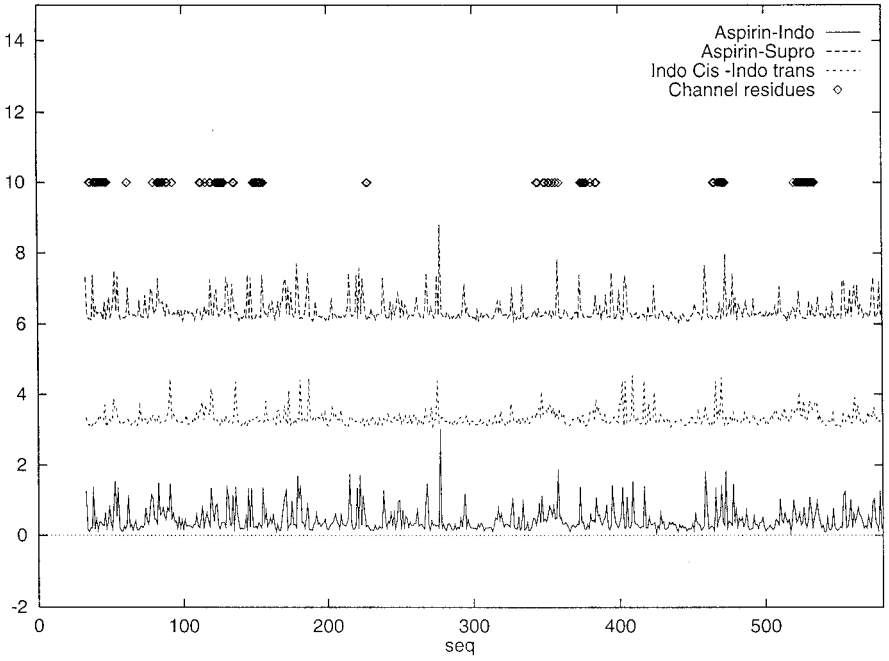

Figure 7. Mean factor differences in RMS between inhibited bromoaspirin and iodoindomethacin PGHS-1 complexes (———), between inhibited bromoaspirin and iodosuprofen PGHS-1 complexes (.....), and between *cis* and *trans* iodoindomethacin PGHS-1 complexes (- - -). The residue number is plotted along the abcissa and ΔRMS (Å^2) along the ordinate.

bromoaspirin complex does not appear large enough to accommodate the indomethacin.

Figure 7 provides plots of the difference in RMS between inhibited bromoaspirin and iodoindomethacin PGHS-1 complexes, between inhibited bromoaspirin and iodosuprofen PGHS-1 complexes, and between *cis* and *trans* iodoindomethacin PGHS-1 complexes. It is interesting that the greatest structural variability is located in the regions surrounding the Lys^{222}, and Arg^{277} residues, on a loop above the peroxidase active site. There are slight differences between the *cis* and *trans* iodoindomethacin-PGHS-1 complexes.

We have modeled equally likely binding modes for iodoindomethacin, corresponding to the *cis*-indomethacin, using the AutoDock program. AutoDock randomly manipulates a ligand with the aim of determining its most favourable bound conformation and orientation in the enzyme or receptor. In this case the cluster of similar conformations with the lowest energy corresponded to the crystallographic mode of binding. This structure was energy minimized in the binding site, and the interactions were evaluated.

The program GRID was applied to the active site of the X-ray crystal structure of the ovine PGHS-1 from the iodoindomethacin complex, with the first binding mode in the absence of the inhibitor. A phenol hydroxy (OH), an sp^2 NH group (NH=) and a methyl (C3) probe were used to map key hydrogen-bonding and van der Waals interaction sites. A detailed examination of the 3D regions in the active site of the PGHS-1 at which the GRID probes would interact most selectively with the enzyme (Figure 8) shows that indomethacin fills the entire hydrophobic channel from Tyr^{385} downward a distance of roughly 12–14 Å (black region), forms a salt bridge with Arg^{120} (grey region), and appears to form a hydrogen bond to the hydroxyl of Tyr^{355} with the ester oxygen of the methoxy group (grey and black region). The benzoyl group is stabilized by hydrophobic interactions with Leu^{384}, Tyr^{385}, and Phe^{381}. The benzoyl oxygen interacts with the side chain hydroxyl of Ser^{530} (grey and black region). The indole ring interacts with Val^{349} and Ser^{353}. Additional contacts are made with the amino acid residues Met^{113}, Val^{116}, Ile^{523}, and Ala^{527} (light grey region). It has been known from the binding studies [29] that these interactions produce significant effects on the binding affinity.

Finally, in the initial molecular modeling studies, the enzyme crystal structure of the PGHS-1/bromoaspirin and PGHS-1/iodosuprofen complexes

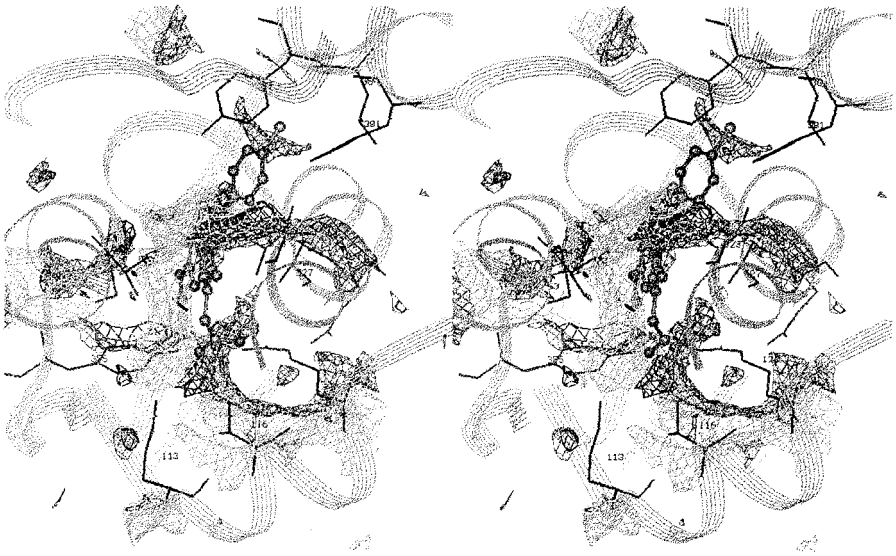

Figure 8. Docking the indomethacin inhibitor in the cyclooxygenase active site channel in ovine PGHS-1 (in stereoview). Only residues in close contact with the ligand are shown. The regions represent the positions at which the GRID probes would interact most selectively with the enzyme. The contours at −2.0 kcal/mol (light grey), at −3.0 kcal/mol (grey) and at −3.0 kcal/mol (black) are given for the GRID calculations carried out for the enzyme structure from the iodoindomethacin/PGHS-1 complex using methyl, phenolic hydroxyl and sp^2 NH probes, respectively.

was used in docking diclofenac and fenamates, respectively.

GRID force field

The GRID method uses probes to determine favourable interaction sites on the surface of a molecule. To assist the elucidation of the time-dependent binding mode, the GRID program was applied to the active site of the X-ray crystal structure of the ovine PGHS-1 from the iodosuprofen, bromoaspirin and iodoindomethacin complexes, respectively [11], with the first binding mode in the absence of the inhibitor (Figures 8 and 9). Thus, GRID mapped the highlighted interaction site differences between the prime sides. The methyl probe produced a completely filled contour at −2.0 kcal/mol on the prime site, indicating that the center of this region had reduced van der Waals contact. The OH and NH= probes, contoured at −3.0 kcal/mol, mapped polar interaction sites, including a large area bordering Arg^{120}, Glu^{524}, and Tyr^{355}, and the approximate locations of Tyr^{385}, Ser^{530}, and Ser^{353} residues.

Docking studies

The results of the set of docking experiments are summarized in Table 3. In all cases except niflumic and clonixin, the best solution was energetically well-separated from the less favorable conformations.

Table 3. Results of simulated-annealing docking

Compound	Number in rank	Lowest energy (kcal/mol)
Clonixin	6	−32.8
Diclofenac	22	−22.8
Flufenamic	42	−29.3
Indomethacin	20	13.6
Mefenamic	32	−31.8
Meclofenamic	38	−27.8
Niflumic	2	−30.0

The results of docking seven receptor-ligand complexes (Table 4) show the carboxylic acid group of NSAIDs located in a favourable position for interacting with the guanidinium group of Arg^{120}, which facilitates the formation of a salt bridge with Arg^{120}.

The positively charged guanidinium group of Arg^{120} of PGHS-1 interacts with the negative long-range electrostatic potential in the region surrounding the carboxylic group of acid NSAIDs. This ionic interaction may be essential for the formation of a tight binding inhibitor complex leading to the time-

Table 4. The main residues in contact with the ligand, and the smallest distance (R, in Å) between an atom of the residue and any atom of the ligand

Compound	R (Å)						
	Arg^{120}	Ser^{353}	Val^{349}	Tyr^{355}	Ile^{523}	Ser^{530}	Ala^{527}
Clonixin	3.0	2.8	2.7	4.2	6.8	3.0	2.9
Diclofenac	3.4	1.4	2.6	1.4	1.6	2.4	3.2
Flufenamic	2.6	3.3	3.0	4.1	5.4	4.6	3.5
Indomethacin	3.4	4.4	1.6	1.7	1.4	3.4	1.5
Mefenamic	2.7	3.1	2.8	4.7	5.3	6.1	2.8
Meclofenamic	2.5	2.1	3.6	2.5	2.0	2.4	2.4
Niflumic	2.8	3.0	3.0	4.6	5.1	3.9	2.9

dependent inhibition of PGHS by indomethacin, diclofenac and meclofenamic. Only diclofenac shows the carboxylic acid group located in a favourable position for interaction with the hydroxyl of Tyr^{355} and appears to form a hydrogen bond with the residue. With the mutation of the arginine residue ($Arg^{120} \rightarrow Glu$), the acid NSAIDs should show a reduced inhibitory potency against hPGHS-1, but only diclofenac does not alter the basic mechanism of time-dependent inhibition [30].

In the model for indomethacin binding, the chlorophenyl group lies in a hydrophobic pocket at the top of the channel, the carbonyl group is situated within 3.4 Å of Ser^{530}, a potential hydrogen bond donor, and the indole ring is in contact with several aliphatic side chains, including Val^{349}, Ala^{527}, Leu^{531} and Ile^{523}. The *o*-methoxy group interacts closely with main-chain atoms of Tyr^{355} and Ser^{353}. The van der Waals interactions between atoms of the hydrophobic residues Val^{349}, $Ileu^{523}$and Ala^{527}, and atoms of the other time-dependent ligands suggest that the other electrostatic potential topological characteristic required for a tight binding is a positive long-range electrostatic potential in the region surrounding the C9, C10 and C13 atoms.

The time-dependent inhibitor compounds interact closely with main-chain atoms of Leu^{352} and Ser^{353}, in the zones surrounding the first aromatic ring for meclofenamic and diclofenac, or indole ring for the indomethacin. The additional contacts of the benzoyl oxygen or the *ortho* substituents attached to the distal aryl ring are with Ser^{530} and Val^{349}, suggesting that these atoms enhance the time-dependent affinity for PGHS-1.

In studies using EPR spectroscopy [31,32] indomethacin has been found to cause the structural changes in the synthase tyrosyl radical (Tyr^{385}) and in our studies only this compound shows the extended contact surface with the residue Tyr^{385} ($S = 37.7$ $Å^2$, $R = 2.6$ Å). Only flufenamic, clonixin and niflumic present close contacts between atoms and the hydrophobic residues Phe^{518}, Leu^{352} and Val^{116} (Figure 9).

In addition, the program GRID was used to calculate the favourable binding sites on each of the seven compounds. This choice of probes was influenced by the presence of such residues in the active site.

The OH (contour at -5.0 kcal/mol) and N2= (contour at -5.0 kcal/mol) probes (Figures 10, 11 and 12) mapped the favourable interaction sites for the hydrogen and ionic bonds, which included a large area bordering the carboxylic acid group, and produced contrasting maps between time-dependent and time-independent inhibitors.

In the former case, a large binding contour was observed in the upper and middle zones, around the amino group and the first aromatic ring or indole ring. The methyl probe produced a completely filled contour at -2.0 kcal/mol on the prime side, while the upper area was a torus, indicating that the center of this region had reduced van der Waals contact. Only the time-dependent inhibitors showed a large hydrophobic area bordering the second aromaric ring.

QSAR

To determine the ionic interaction between the anionic carboxylic group of acid NSAIDs with the monocationic guanidinum group of the Arg^{120} residue in the active site conformations, the ab initio (3–21G* level) reaction enthalpies for the formation of an ionic bond with a completely protonated guanidinum group were

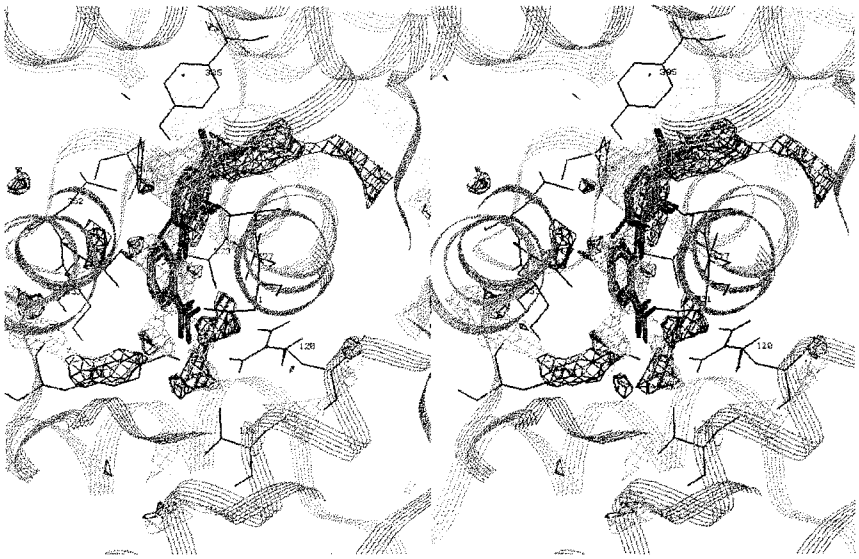

Figure 9. Docking the fenamate inhibitors in the cyclooxygenase active site channel in ovine PGHS-1 (in stereoview). Only residues in close contact with the ligand are shown. The regions represent the positions at which the GRID probes would interact most selectively with the enzyme. The contours at −2.0 kcal/mol (light grey), at −3.0 kcal/mol (grey) and at −3.0 kcal/mol (black) are given for the GRID calculations carried out for the enzyme structure from the bromoaspirin/PGHS-1 complex using methyl, phenolic hydroxyl and sp^2 NH probes, respectively.

calculated with geometry optimization. To determine the disorder in the arrangement of the water molecules when they surround a compound, the free energy of solvation was calculated.

The reaction enthalpies (ΔH_r), free energies of solvation in aqueous solution ($\Delta G_{solvation}$) and molecular volumes are reported in Table 5.

The efficiency of inhibition (lower K_I^*) associated with a stabilization of the complex EI^*, increased when the magnitude of interaction with Arg^{120} (ΔH_r) increased. In the internal medium the cationic-anionic interaction lasts only a fraction of a second because of the quantity of ionic salts present and the possibility this offers for ion exchange. However, if this bond is reinforced, as is assumed, through the simultaneous presence of other interactions (hydrophobic, hydrogen bonding, van der Waals), it becomes much stronger and is able to last much longer.

However, strong binding of the carboxylate group of inhibitors is an important characteristic of time-dependent inhibition; the methyl esters of the time-dependent inhibitor fenamates were totally devoid of time-dependent properties. Diclofenac and meclofenamic acid retained some inhibitory effects (potency was decreased 50–100 fold) against the mutation of PGHS-1 ($Arg^{120} \rightarrow$ Glu); in contrast, no significant inhibition of hPGHS-1 was observed with indomethacin. The time-dependent inhibition by diclofenac is similar for the mutant PGHS-1 albeit at a higher concentration of inhibitor [30]. The rate constant for the forward isomerization, k_2, into the complex EI^*, increased when a contact surface with Ser^{530} increased.

The energies for the formation (ΔH_r) of a salt bridge with Arg^{120}, free energy of solvation ($\Delta G_{solvation}$) and molecular volume are consistent with those obtained using molecular modeling.

The equation obtained was

$$\mathrm{Log}(1/\mathrm{IC}_{50}) = -34.81 - 0.1635\Delta H_r - 0.241\Delta G_{solvation}$$

$$Q^2 = 0.74,\ \mathrm{SDEP} = 0.2,\ R^2 = 0.81,\ F = 22.0$$

Discussion

The cyclooxygenase active site consists of a long, narrow, hydrophobic channel and the presence of Arg^{120} at the mouth of the channel provides a suitable moiety providing a ligand to the carboxylate group [29]. The active compounds present the topological MEP characteristics (Figures 4, 5 and 6) necessary for PGHS-1 recognition: two very deep negative zones around the carboxylic oxygen atoms.

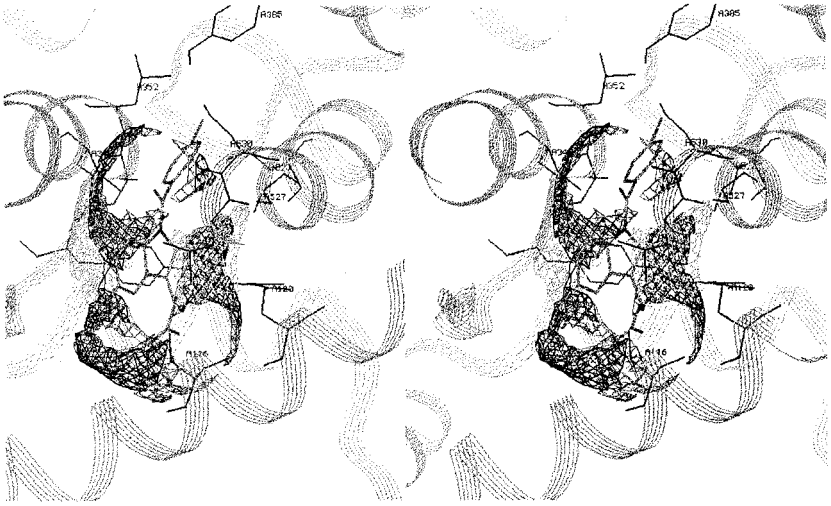

Figure 10. Docking the indomethacin inhibitor in the cyclooxygenase active site channel in ovine PGHS-1 (in stereoview). Only residues in close contact with the ligand are shown. The regions represent the positions at which the GRID probes would interact most selectively with the indomethacin. The contours at −2.0 kcal/mol (light grey), at −5.0 kcal/mol (grey) and at −5.0 kcal/mol (black) are given for the GRID calculations carried out for the drug structure using methyl, phenolic hydroxyl and sp^2 NH probes, respectively.

Table 5. Thermodynamic parameters and antiinflammatory activity for the selected compounds

Compound	COO^-....Arg^{120} (ΔH_r) (kcal/mol)	$\Delta G_{solvation}$ (kcal/mol)	Volume (Å^3)	Log (1/IC_{50}) (a)Log (1/K_I^*)
Clonixin	−111.4527	−65.447	186.41	−1.16
Diclofenac	−116.3874	−68.054	206.47	0.89(a)
Flufenamic	−112.4686	−62.294	184.52	−0.99
Indomethacin	−117.2296	−68.870	259.63	1.11(a)
Mefenamic	−114.7913	−65.848	186.33	−1.26
Meclofenamic	−116.3680	−68.336	206.69	0.97(a)
Niflumic	−107.5552	−64.348	180.52	−1.51

All the active time-dependent compounds show MEPs with a negative conical surface with their vertex on the minimum of the carboxyl group, which extends around the first aromatic ring to the central region, keeping an angle of 61° or larger (Figure 5). The upper right zone shows a bulk of repulsive potential to an approaching electrophile region.

The upper zone seems to be the most discriminant with respect to time-dependent activity. The C9 and C13 substituents of the aromatic ring appear to play a key role. However, as previously shown [33,34] for the arylacetic derivatives, the possibility of electrostatic discrimination is connected not so much to the effect of these groups on the depth of the MEP minimum at N1 as to the overall topology of the MEP distribution in the region of space surrounding the bridging amino group due to the torsion angle between the two aromatic rings and by conferring conformational rigidity to the inhibitor.

Comparison of the inhibitors shows that all kinetic constants (Tables 1 and 2) must be examined in order to understand which factors contribute to the overall efficiency of inhibition. The K_I^* values are similar, although the individual rate constants are vastly different: K_I is seven-fold lower for diclofenac and k_2 is twelve-fold slower for diclofenac.

The carboxylic acid moiety of all inhibitors forms a salt bridge with the Arg^{120} residue, the two carboxylate oxygen atoms of the inhibitor lying between 1.45 and 1.60 Å from one of the guanidino nitrogens of the arginine, and the ionic bond enthalpies showed a significant influence on the overall inhibitory effect.

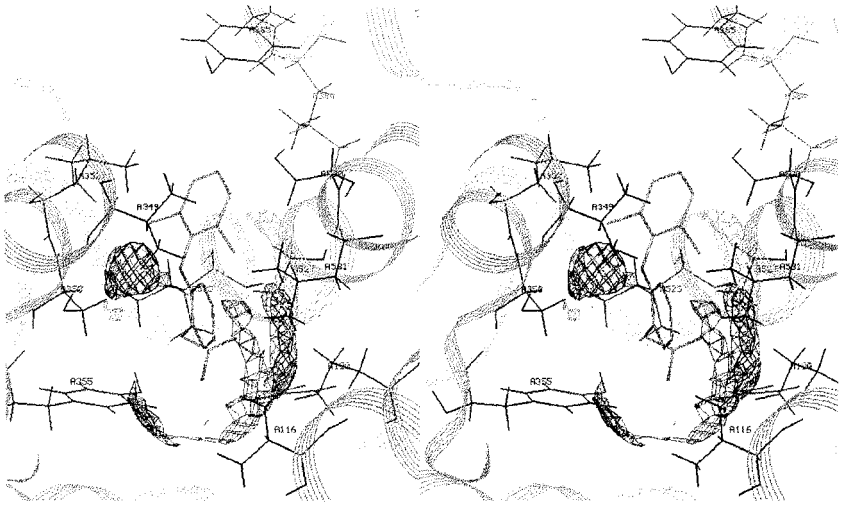

Figure 11. Docking the diclofenac inhibitor in the cyclooxygenase active site channel in ovine PGHS-1 (in stereoview). Only residues in close contact with the ligand are shown. The regions represent the positions at which the GRID probes would interact most selectively with the diclofenac. The contours at −2.0 kcal/mol (light grey), at −5.0 kcal/mol (grey) and at −5.0 kcal/mol (black) are given for the GRID calculations carried out for the enzyme structure from the iodoindomethacin/PGHS-1 complex using methyl, phenolic hydroxyl and sp^2 NH probes, respectively.

In addition, one carboxylic acid oxygen of diclofenac (1.4 Å) and indomethacin (1.7 Å) lies < 2.0 Å from the phenolic hydroxyl of Tyr^{355}, evidently forming a hydrogen bond; side chains lining the channel below the inhibitor surround it and render it inaccessible to solvent.

The k_2 and k_{-2} values suggest that the interactions that promote the slow binding kinetics must be examined in order to understand the contact surfaces between the ligand atoms and atoms of the Ser^{530}, Ser^{353}, and $Ileu^{523}$ residues. A hydrogen bond also appears to be formed between the carbonyl bridge oxygen of indomethacin and the side chain hydroxyl of Ser^{530}: the two atoms are separated by 3.4 Å, and display a favourable geometry for hydrogen bonding (Figure 10). The contact surfaces (Figures 11 and 12) between the ligand atoms and atoms of the Ser^{530} and $Ileu^{523}$ residues were increased for indomethacin (46.0 and 53.9 $Å^2$) and meclofenamic (41.3 and 32.5 $Å^2$) versus diclofenac (38.6 and 35.8 $Å^2$), while the contact surfaces between the ligand atoms and atoms of the Ser^{353} residue in the zones surrounding the first aromatic ring were increased for diclofenac (45.7 $Å^2$). The second phenyl ring establishes the van der Waals interactions with a number of hydrophobic side chains lining the channel, including Val^{349}, Ala^{527}, Leu^{531} and Ile^{523}. Presumably indomethacin, diclofenac and meclofenamic cause the enzyme to undergo a subtle conformational change to a form that binds compounds even more tightly.

Limited proteolysis experiments provide direct evidence that these time-dependent inhibitors were found to block access of proteases to the Arg^{277} region; flufenamate also protected the synthase against attack by trypsin although not to the degree observed with indomethacin; the effectiveness of protection depends upon the tightness of binding as well as the bulk and orientation of the bound NSAID [3].

Similar experiments conducted with a potent time-dependent cyclooxygenase inhibitor, in an attempt to protect apoPGH synthase from tryptic cleavage at Arg^{277} [35], have shown that time-dependent inhibition mechanisms induce a conformational change in the PGHS protein [36,37].

Conclusions

This paper is a further development of the indirect theoretical approach to the study of the time-dependent PGHS-1 inhibitors and their interactions with the receptor. On the basis of the 3D MEP representations considered, significant electrostatic dissimilarities were detected between time-dependent inhibitors and simplified competitive inhibitors. The space around the R1-substituent of the phenyl ring appears to play a key role. From the X-ray crystal-

Figure 12. Docking the fenamate inhibitors in the cyclooxygenase active site channel in ovine PGHS-1 (in stereoview). Only residues in close contact with the ligand are shown. The regions represent the positions at which the GRID probes would interact most selectively with the fenamates. The contours at −2.0 kcal/mol (light grey), at −5.0 kcal/mol (grey) and at −5.0 kcal/mol (black) are given for the GRID calculations carried out for the drug structure using methyl, phenolic hydroxyl and sp^2 NH probes, respectively. The solid surface represents the positions at which the probes would interact selectively with the meclofenamic acid.

lographic binding studies it has been possible to use a structure-based ligand design strategy to determine which interactions make a significant contribution to the biological activity. This study shows that the use of the program combination Grid/AutoDock may provide an objective method of obtaining similar information.

The K_I^* and IC_{50} values suggest that the interactions that promote the slow binding kinetics must be examined in order to calculate the reaction energies for the formation of a salt bridge between the deprotonated carboxylic acid group of acid NSAIDs with the monocationic guanidinum group of Arg^{120}.

All the active time-dependent compounds show the lowest free energies of solvation in aqueous solution, and the maximum molecular volumes. Indomethacin, diclofenac and meclofenamic cause the enzyme to undergo a subtle conformational change to a form that binds the compound even more tightly, with slight structural changes confined to reorientations of the Arg^{277} and Gln^{358} side chains.

These results show that the model has reliably chosen regions of biological significance consistent with both the X-ray crystallographic and kinetic results.

Acknowledgements

The authors thank Dr. V. Trigueros for ovine seminal vesicles samples, Dra. Blanca Barrera for the Clonixin samples, Dr. M.M. Garrett for his software AutoDock v. 2.4, and J. Luque for valued assistance. R. Pouplana acknowledges the Fundaciò Catalana per la Recerca for providing computational support in ab initio calculations. Financial support by the Spanish FIS is gratefully acknowledged (Grant 94/995).

References

1. Earnest, D.L., Hixson, L.J. and Alberts, D.S., J. Cell. Biochem. Suppl., 161 (1992) 156.
2. Kargman, S.L., O'Neill, G.P., Vickers, P.J., Evans, J.F., Mancini, J.A. and Jothy, S., Cancer Res., 55 (1995) 2556.
3. Smith, W.L., Marnett, L.J. and DeWitt, D.L., In Taylor, C.W. (Ed.) Pharmacological Therapy, Vol. 49, Pergamon Press, London, 1991, pp. 153–179.
4. Lecomte, M., Laneuville, O., Ji, C., DeWitt, D.L. and Smith, W.L., J. Biol. Chem., 269 (1994) 13207.
5. Kulmacz, R.J. and Wang, L.-H., J. Biol. Chem., 270 (1995) 24019.
6. Barnett, J., Chow, J., Ives, D., Chiou, M., Mackenzie, R., Osen, E., Nguyen, B., Tsing, S., Bach, C., Freire, J., Chan, H., Sigal, E. and Ramesha, C., Biochim. Biophys. Acta, 1209 (1994) 130.
7. Ouellet, M. and Percival, D., Biochem. J., 306 (1995) 247.

8. Scherrer, A., In Rainsford, K.D. and Path, M.R.C. (Eds.) Anti-Inflammatory and Anti-Rheumatic Drugs, Vol. 2, CRC Press, Boca Raton, FL, 1985, pp. 65–85.
9. Picot, D., Loll, P.J. and Garavito, R.M., Nature, 367 (1994) 243.
10. Loll, P.J., Picot, D. and Garavito, R.M., Nature Struct. Biol., 2 (1995) 637.
11. Loll, P.J., Picot, D., Ekabo, O. and Garavito, R.M., Biochemistry, 35 (1996) 7330.
12. Kulmacz, R.J. and Lands, W.E.M., In Benedetto, C., McDonald Gibson, R.G., Nigam, S. and Slater, T.F. (Eds.), Prostaglandin and Related Substances: A Practical Approach, IRL Press, Washington, DC, 1987, pp. 209–227.
13. Watnick, A.S., Taber, R.I. and Tabachnick, I.A., Arch. Int. Pharmacodyn., 190 (1971) 78.
14. Callan, O.H., On-Yee, S. and Swinney, D.C., J. Biol. Chem., 271 (1996) 3548.
15. Lozano, J.J., Pouplana, R., López, M. and Ruiz, J., J. Mol. Struct. (Theochem), 335 (1995) 215.
16. Moser, P., Sallmann, A. and Wiesenberg, I., J. Med. Chem., 33 (1990) 2358.
17. Dhanaraj, V. and Vijayan, M., Acta Crystallogr., B44 (1988) 406.
18. Biosym Technologies, Inc., San Diego, CA.
19. Kollman, P.A., J. Comput. Chem., 11 (1990) 431.
20. AMSOL 5.4.1., Oxford Molecular Group.
21. Frisch, M.J., Head-Gordon, M., Trucks, G.W., Foresman, J.B., Schlegel, H.B., Raghavachari, K., Robb, M.A., Binkley, J.S., Gonzalez, C., Defrees, D.J., Fox, D.J., Whiteside, R.A., Seeger, R., Melius, C.F., Baker, J., Martin, R.L., Kahn, L.R., Stewart, J.J.P., Topiol, S. and Pople, J.A., Gaussian 92, Gaussian Inc., Pittsburgh, PA, 1992.
22. Sanz, F., Manaut, F., Segura, J.J., Carbó, M. and De la Torre, R., J. Mol. Struct. (Theochem), 170 (1988) 171.
23. Sobolev, V., Wade, R.C., Vriend, G. and Edelman, M., Proteins Struct. Funct. Genet., 25 (1996) 120.
24. GRID v.15, Molecular Discovery Ltd., Elms Parade, Oxford, 1997.
25. Goodford, P.J., J. Med. Chem., 28 (1985) 849.
26. Kulmacz, R.J., Pendleton, R.B. and Lands, W.E.M., J. Biol. Chem., 269 (1994) 5527.
27. Ferenczy, G.G., Reynolds, C.A. and Richards, W.G., J. Comput. Chem., 11 (1990) 159.
28. Lozano, J.J., López, M., Ruiz, J., Vazquez, I.J. and Pouplana, R., In Wermuth, C.G. (Ed.) Trends in QSAR and Molecular Modelling'92, ESCOM, Leiden, 1993, pp. 560–562.
29. Bhattacharyya, D.K., Lecomte, M., Rieke, C.J., Garavito, M. and Smith, W.L., J. Biol. Chem., 271 (1996) 2179.
30. Mancini, J.A., Riendeau, D., Falgueyret, J.P., Vickers, P.J. and O'Neill, G.P., J. Biol. Chem., 270 (1995) 29372.
31. Kulmacz, R.J., Palmer, G. and Ah-Lim, T., Mol. Pharm., 40 (1991) 833.
32. Ah-Lim, T., Kulmacz, R.J. and Palmer, G., J. Biol. Chem., 270 (1995) 10503.
33. Ruiz, J., López, M., Milà, J., Lozoya, E., Lozano, J.J. and Pouplana, R., J. Comput.-Aided Mol. Design, 7 (1993) 183.
34. López, M., Lozoya, E., Ruiz, J., Milà, J. and Pouplana, R.A., In Silippo, C. and Vittoria, A. (Eds.) QSAR: Rational Approaches to the Design of Bioactive Compounds, Elsevier, Amsterdam, 1991, pp. 315–318.
35. Mitchell, J.A., Akarasereenont, P., Thiemermann, C., Flower, R.J. and Vane, J.R., Proc. Natl. Acad. Sci. USA, 90 (1994) 11693.
36. Meade, E.A., Smith, W.L. and DeWitt, D.L., J. Biol. Chem., 268 (1993) 6610.
37. Kurumbail, R.G., Stevens, A.M., Gierse, J.K., McDonald, J.J., Stegeman, R.A., Pak, J.Y., Gildehaus, D., Miyashiro, J.M., Penning, T.D., Seibert, K., Isakson, P.C. and Stallings, W.C., Nature, 384 (1996) 644.
38. Kulmacz, R.J. and Lands, W.E.M., J. Biol. Chem., 260 (1985) 12572.